Spectrochimica Acta Part A: Molecular and Biomolecular Spectroscopy 200 (2018) 290–297

Contents lists available at ScienceDirect

Spectrochimica Acta Part A: Molecular and Biomolecular Spectroscopy

journal homepage: www.elsevier.com/locate/saa

An analytical formula for predicting R-branch high-lying transition lines of BiLi molecule

Qunchao Fan [a], Chuping Hu [a], Jia Fu [a,*], Jie Ma [b,*], Zhixiang Fan [a], Yonggen Xu [a,*], Huidong Li [a], Yi Zhang [c]

[a] School of Science, Key Laboratory of High Performance Scientific Computation, Xihua University, Chengdu 610039, China
[b] State Key Laboratory of Quantum Optics and Quantum Optics Devices, Laser Spectroscopy Laboratory, College of Physics and Electronics Engineering, Shanxi University, Taiyuan 030006, China
[c] College of OptoElectronic Science and Engineering, National University of Defense Technology, Changsha 410073, China

ARTICLE INFO

Article history:
Received 15 January 2018
Received in revised form 29 March 2018
Accepted 30 March 2018
Available online 10 April 2018

Keywords:
BiLi
Transitional spectral lines
R-branch
Difference converging method

ABSTRACT

A concise and convenient analytical formula without any spectral constant is derived from the conventional expression of R-branch transitional energies for calculating the R-branch high-lying rovibrational emission spectral lines of diatomic molecule. This is based on the thought of Sun's difference converging method (DCM) in 2011. This formula can correctly predict the high-lying transitional emission spectral lines only using 11 known experimental transition lines and a set of physical criteria when any spectral constants of the system are not available. Furthermore, a new method for analyzing the accuracy of prediction with the improved formula is proposed, which point out the core problem of the predicted spectrum and give a quantitative conclusion on the reliability of our work. In this work, the new method is applied to study the R-branch transitional emission spectra of the (0–0) band of the $A_20^+ \rightarrow X_10^+$ and $A_20^+ \rightarrow X_21$ transition systems of BiLi molecule. A series of experimental and theoretical comparisons and discussions show that under the condition of lack of any spectral constants, our method can still use 11 known experimental transition spectral data to reproduce the R-branch emission spectral lines reliably including the high excited rovibrational transition spectral lines.

1. Introduction

The rovibrational transition lines and the rovibrational energies are important quantities in the field of molecular physics and laser spectroscopy [1,2]. These physical quantities play very important roles in the study of molecular structures and molecular properties [3–7], such as research on the molecular fluorescence radiations [8], the cold atomic and molecular physics [9–11]. In recent years, there are many experimental techniques [12–15] and theoretical calculations [16,17] have been introduced to obtain accurate molecular transition lines. However, the spectral data for the low excitation rotation quantum states of the system can be obtained well, the accurate R-branch high-lying transition lines are still difficult to obtain, this fact greatly affected the molecular structures and chemical reactions in-depth development.

In our previous work, an analytical formula was proposed to predict the P-branch high-lying transition spectral lines by taking multiple spectral differences of molecular total energy [18]. The method indicates that as long as 15 known experimental transition lines together with some low-order spectral constants such as $\{B_{v'}, B_{v''}, D_{v'}, D_{v''}\}$, the formula can calculate the results of the unknown P-branch high-lying rovibrational emission spectral lines. And then, in 2016, Sun et al. [19]. reconsidered the influence of the high order constant H_v that is neglected in previous expression and obtained a new formula, which was superior to the previous P-branch results. However, there is a drawback of the new formula that is necessary to obtain 15 experimental spectral data and experimental rotational spectral constants such as $\{D_{v''}, D_{v'}, H_{v''}, H_{v'}\}$, the high order rotational spectral constants are still very lacking for some systems. In order to solve this problem, a more concise and convenient analytical formula than our previous formula is derived to calculate the R-branch high-lying rovibrational emission spectral lines for diatomic molecule based on the thought of Sun's difference converging method, we still call it the difference converging method (DCM) in this work.

Elaborate studies have been carried out experimentally and theoretically for one to understand the electronic structures and properties of the gaseous BiLi molecule [20,21] and Bi-Li compounds [22–24]. However, due to the limitations of experimental equipment and theoretical methods, the correct structures of BiLi molecule especially the high-lying excitation rotational quantum states are still not available. In this paper, Using the improved new formula, the R-branch high-lying transition emission spectral lines of the (0–0) band of the $A_20^+ \rightarrow X_10^+$ and $A_20^+ \rightarrow X_21$ systems of BiLi molecule are studied. Section 2 presents the new formula derivations. Section 3 is the results and discussions. Section 4 summarizes this study.

* Corresponding author.
E-mail addresses: fujiayouxiang@126.com (J. Fu), mj@sxu.edu.cn (J. Ma), xuyg@mail.xhu.edu.cn (Y. Xu).

https://doi.org/10.1016/j.saa.2018.03.082
1386-1425/

2. An Analytical Formula for R-branch Transition Lines

The following derivation process is still based on the idea of differentiation proposed in our previous work [18]. Starting from the classical expressions of total transition line for a diatomic system, the R-branch ($\Delta J = +1$) transition spectral lines containing high-order rotational constant L_v for a diatomic molecule can be expressed as [25].

$$\begin{aligned}\nu &= \nu_0 + (J+1)[B_{v'}(J+2) - B_{v''}J] - (J+1)^2\left[D_{v'}(J+2)^2 - D_{v''}J^2\right] \\ &+ (J+1)^3\left[H_{v'}(J+2)^3 - H_{v''}J^3\right] + (J+1)^4\left[L_{v'}(J+2)^4 - L_{v''}J^4\right] + \cdots\end{aligned} \tag{1}$$

where J is rotational quantum number, $\{L_{v'}, L_{v''}, H_{v'}, H_{v''}, D_{v'}, D_{v''}, B_{v'}, B_{v''}\}$ are the rotation spectral constants corresponding to different vibrational quantum number v [25]. Following derivations are based on the Eq. (1) and multiple energy (transition line) differences. The second transition line difference (but the third energy difference) between four rotational states J_1, J_2, J_3, and J_4 are

$$\begin{aligned}&(\nu_{J_1} - \nu_{J_2}) - (\nu_{J_3} - \nu_{J_4}) \\ &= B_{v'}[(J_1+1)(J_1+2) - (J_2+1)(J_2+2) - (J_3+1)(J_3+2) + (J_4+1)(J_4+2)] \\ &\quad - B_{v''}[(J_1+1)J_1 - (J_2+1)J_2 - (J_3+1)J_3 + (J_4+1)J_4] \\ &- D_{v'}\left[(J_1+1)^2(J_1+2)^2 - (J_2+1)^2(J_2+2)^2 - (J_3+1)^2(J_3+2)^2 + (J_4+1)^2(J_4+2)^2\right] \\ &\quad + D_{v''}\left[(J_1+1)^2{J_1}^2 - (J_2+1)^2{J_2}^2 - (J_3+1)^2{J_3}^2 + (J_4+1)^2{J_4}^2\right] \\ &+ H_{v'}\left[(J_1+1)^3(J_1+2)^3 - (J_2+1)^3(J_2+2)^3 - (J_3+1)^3(J_3+2)^3 + (J_4+1)^3(J_4+2)^3\right] \\ &\quad - H_{v''}\left[(J_1+1)^3{J_1}^3 - (J_2+1)^3{J_2}^3 - (J_3+1)^3{J_3}^3 + (J_4+1)^3{J_4}^3\right] \\ &+ L_{v'}\left[(J_1+1)^4(J_1+2)^4 - (J_2+1)^4(J_2+2)^4 - (J_3+1)^4(J_3+2)^4 + (J_4+1)^4(J_4+2)^4\right] \\ &\quad - L_{v''}\left[(J_1+1)^4{J_1}^4 - (J_2+1)^4{J_2}^4 - (J_3+1)^4{J_3}^4 + (J_4+1)^4{J_4}^4\right]\end{aligned} \tag{2}$$

Eq. (2) may also be written as

$$\begin{aligned}(\nu_{J_1} - \nu_{J_2}) - (\nu_{J_3} - \nu_{J_4}) &= B_{v'}a_1(J_1 \sim J_4) - B_{v''}a_2(J_1 \sim J_4) - D_{v'}a_3(J_1 \sim J_4) + D_{v''}a_4(J_1 \sim J_4) \\ &+ H_{v'}a_5(J_1 \sim J_4) - H_{v''}a_6(J_1 \sim J_4) + L_{v'}a_7(J_1 \sim J_4) - L_{v''}a_8(J_1 \sim J_4)\end{aligned}$$

Therefore, the rotational constant $L_{v''}$ may be given from above formula as

$$\begin{aligned}L_{v''} &= -\frac{(\nu_{J_1} - \nu_{J_2} - \nu_{J_3} + \nu_{J_4})}{a_8(J_1 \sim J_4)} + B_{v'}\frac{a_1(J_1 \sim J_4)}{a_8(J_1 \sim J_4)} - B_{v''}\frac{a_2(J_1 \sim J_4)}{a_8(J_1 \sim J_4)} - D_{v'}\frac{a_3(J_1 \sim J_4)}{a_8(J_1 \sim J_4)} \\ &+ D_{v''}\frac{a_4(J_1 \sim J_4)}{a_8(J_1 \sim J_4)} + H_{v'}\frac{a_5(J_1 \sim J_4)}{a_8(J_1 \sim J_4)} - H_{v''}\frac{a_6(J_1 \sim J_4)}{a_8(J_1 \sim J_4)} + L_{v'}\frac{a_7(J_1 \sim J_4)}{a_8(J_1 \sim J_4)}\end{aligned} \tag{3}$$

where the coefficients $\{a_1, a_2, \ldots, a_8\}$ are Eqs. (A.1a)–(A.1h) in the Appendix of the supplementary material. Eq. (3) can also be written for transition lines $\nu_{J_2} \sim \nu_{J_5}$ of arbitrary rotational states (J_2,J_3,J_4,J_5), namely

$$\begin{aligned}L_{v''} &= -\frac{(\nu_{J_2} - \nu_{J_3} - \nu_{J_4} + \nu_{J_5})}{a_8(J_2 \sim J_5)} + B_{v'}\frac{a_1(J_2 \sim J_5)}{a_8(J_2 \sim J_5)} - B_{v''}\frac{a_2(J_2 \sim J_5)}{a_8(J_2 \sim J_5)} \\ &- D_{v'}\frac{a_3(J_2 \sim J_5)}{a_8(J_2 \sim J_5)} + D_{v''}\frac{a_4(J_2 \sim J_5)}{a_8(J_2 \sim J_5)} + H_{v'}\frac{a_5(J_2 \sim J_5)}{a_8(J_2 \sim J_5)} \\ &- H_{v''}\frac{a_6(J_2 \sim J_5)}{a_8(J_2 \sim J_5)} + L_{v'}\frac{a_7(J_2 \sim J_5)}{a_8(J_2 \sim J_5)}\end{aligned} \tag{4}$$

Eqs. (3) and (4) should be equal, and then one can get $L_{v''}$ expression as

$$\begin{aligned}L_{v'} &= (\nu_{J_1} - \nu_{J_2} - \nu_{J_3} + \nu_{J_4})\, b_1(J_1 \sim J_5) - (\nu_{J_2} - \nu_{J_3} - \nu_{J_4} + \nu_{J_5})\ \ b_2(J_1 \sim J_5) \\ &- B_{v'}\, b_3(J_1 \sim J_5) + B_{v''}\, b_4(J_1 \sim J_5) + D_{v'}\, b_5(J_1 \sim J_5) \\ &- D_{v''}\, b_6(J_1 \sim J_5) - H_{v'}\, b_7(J_1 \sim J_5) + H_{v''}\, b_8(J_1 \sim J_5)\end{aligned} \tag{5}$$

where the coefficients $\{b_1, b_2, \ldots, b_8\}$ can be found in Eqs. (A.3a)–(A.3h). Similarly, Eq. (5) can also be written for arbitrary transition lines $\nu_{J_2} \sim \nu_{J_6}$

$$\begin{aligned}L_{v'} &= (\nu_{J_2} - \nu_{J_3} - \nu_{J_4} + \nu_{J_5})\, b_1(J_2 \sim J_6) - (\nu_{J_3} - \nu_{J_4} - \nu_{J_5} + \nu_{J_6})\, b_2(J_2 \sim J_6) \\ &- B_{v'}\, b_3(J_2 \sim J_6) + B_{v''}\, b_4(J_2 \sim J_6) + D_{v'}\, b_5(J_2 \sim J_6) \\ &- D_{v''}\, b_6(J_2 \sim J_6) - H_{v'}\, b_7(J_2 \sim J_6) + H_{v''}\, b_8(J_2 \sim J_6)\end{aligned} \tag{6}$$

Eqs. (5) and (6) should be equal, so that one can eliminate $L_{v''}$ and get the expression of $H_{v''}$. In this way, all rotation spectral constants $\{L_{v'}, L_{v''}, H_{v'}, L_{v'}, L_{v''}, H_{v'}, H_{v''}, D_{v'}, D_{v''}, B_{v'}, B_{v''}\}$ in Eq. (1) will be eliminate finally, and one can get the following formula expression as

$$\nu_{J_{12}} = \nu_{J_1}C_1 + \nu_{J_2}C_2 + \nu_{J_3}C_3 + \nu_{J_4}C_4 + \nu_{J_5}C_5 + \nu_{J_6}C_6 + \nu_{J_7}C_7 + \nu_{J_8}C_8 + \nu_{J_9}C_9 + \nu_{J_{10}}C_{10} + \nu_{J_{11}}C_{11} \tag{7}$$

where $C_1 \sim C_{11}$ are the expansion coefficients (see the Appendix of the supplementary material). Eq. (7) is the analytical formula without any rotational constants proposed to compute unknown R-branch emission spectral line $\nu_{J_{12}}$ of a rotational state J_{12} only using other 11 known experimental transition lines ($\nu_{J_1} \sim \nu_{J_{11}}$) for a given vibrational transition (v', v'') of a diatomic system. The C_i function is related to the rotational quantum numbers $J_1 \sim J_{12}$. In the

above derivation, no mathematical approximations and physical models are used except that, in rotational energy expansion, the higher order terms of the rotational constants with the order of 10–15 in cm^{-1} and smaller are neglected.

Although it is difficult to get the R-branch high-lying excited transition emission lines for a given transition band of a diatomic system, one can obtain $m(m \geq 11)$ low-lying rovibrational transition lines $[v_J]$ by using some reliable experimental methods such as Fourier-transform spectrometer technology [21]. Therefore, the R-branch transition lines of high-lying excited states for the transition band of the diatomic molecule can be predicted with the m known experimental data $[v_J]$ by using calculate Eq. (7) as the following steps:

(1). Firstly, eleven transition lines will be chosen at a time from the $m(m \geq 11)$ known experimental transition lines, so then there will be at least $N = C_m^{11}$ such selections. Since there is no any physical limitation on the selections, it is only necessary to ensure that the expansion coefficients C are not equal to zero, namely $C_1 \sim C_{11} \neq 0$.

(2). And then, one can substituting each selection (eleven experimental transition lines) in Eq. (7) to calculate unknown transition lines including high-lying transition emission spectral lines.

(3). N sets different calculation results of (m + k) transition lines $[v_{J_1}, v_{J_2}, \ldots, v_{J_m}; v_{J_{m+1}}, v_{J_{m+2}}, \ldots, v_{J_{m+k}}]_{i,\,cal}$ will be obtained finally by using Eq. (7), the (m + k) corresponding rotational quantum numbers $(J_1, \ldots J_m; J_{m+1} \ldots J_k)$ are also given $[v_{J_1}, v_{J_2}, \ldots, v_{J_m}]_{i,\,cal}$. There will always be a set of calculations that best meet the following physical requirements:

$$|\nu_{J,\,\mathrm{expt}} - \nu_{J,cal}| \rightarrow 0 \tag{8}$$

$$|\Delta_{J,\,\mathrm{expt}} - \Delta_{J,cal}| \rightarrow 0, \quad \Delta_J = \nu_{J-1} - \nu_J \tag{9}$$

$$|\Delta_{J,\,\mathrm{expt}}/\nu_{J-1,\,\mathrm{expt}}| - |\Delta_{J,cal}/\nu_{J-1,cal}| \rightarrow 0 \tag{10}$$

where $|\nu_{J,\mathrm{expt}} - \nu_{J,\,cal}|$ is the difference between experimental and theoretical values, the $\Delta_J = \nu_{J-1} - \nu_J$ is the first spectral difference, the $|\Delta_{J,\mathrm{expt}} - \Delta_{J,\,cal}|$ is the difference between the first spectral difference of the experimental values and the first spectral difference of the theoretical calculation. Therefore, the best transition spectral lines combination $[v_i]$ satisfying the physical criterion Eqs. (8)–(10) are found for commendably revealing the true physical information of the transitional lines. The results show that they not only exactly reproduce the m experimental data $[v_{J_1}, v_{J_2}, \ldots, v_{J_m}]_{i,\,cal}$, but also correctly predict the high-lying transitional lines $[v_{J_{m+1}}, v_{J_{m+2}}, \ldots, v_{J_{m+k}}]_{i,\,cal}$.

Unavoidably, there is a certain error Δv_{J_1} between the experimental values and the real values, therefore, Eq. (7) becomes

$$\begin{aligned} \nu'_{J_{12}} = {} & (\nu_{J_1} + \Delta\nu_{J_1})C_1 + (\nu_{J_2} + \Delta\nu_{J_2})C_2 + (\nu_{J_3} + \Delta\nu_{J_3})C_3 + (\nu_{J_4} + \Delta\nu_{J_4})C_4 \\ & + (\nu_{J_5} + \Delta\nu_{J_5})C_5 + (\nu_{J_6} + \Delta\nu_{J_6})C_6 + (\nu_{J_7} + \Delta\nu_{J_7})C_7 + (\nu_{J_8} + \Delta\nu_{J_8})C_8 \\ & + (\nu_{J_9} + \Delta\nu_{J_9})C_9 + (\nu_{J_{10}} + \Delta\nu_{J_{10}})C_{10} + (\nu_{J_{11}} + \Delta\nu_{J_{11}})C_{11} \end{aligned} \tag{11}$$

where $\Delta v_{J_i} (i = 1,2,\cdots,11)$ are the error introduced by experiment. Compare Eq. (7) with Eq. (11), the prediction error caused by experimental uncertainty is

$$\begin{aligned} \Delta\delta = {} & C_1\Delta\nu_{J_1} + C_2\Delta\nu_{J_2} + C_3\Delta\nu_{J_3} + C_4\Delta\nu_{J_4} + C_5\Delta\nu_{J_5} + C_6\Delta\nu_{J_6} \\ & + C_7\Delta\nu_{J_7} + C_8\Delta\nu_{J_8} + C_9\Delta\nu_{J_9} + C_{10}\Delta\nu_{J_{10}} + C_{11}\Delta\nu_{J_{11}} \end{aligned} \tag{12}$$

Notice that all experimental spectrum lines can be predicted by Eq. (11). It is assumed that the error of the calculated value is primarily caused by experimental uncertainty of the selected 11 transition lines and can be estimated by Eq. (12). Thus, if these are $m > 11$ known experimental transition lines, there will be m linear equations:

$$\begin{aligned} \Delta\delta_j = \nu_j^{cal} - \nu_j^{\exp} = {} & C_1(j)\Delta\nu_{J_1} + C_2(j)\Delta\nu_{J_2} + C_3(j)\Delta_{J_3} + C_4(j)\Delta\nu_{J_4} \\ & + C_5(j)\Delta\nu_{J_5} + C_6(j)\Delta\nu_{J_6} + C_7(j)\Delta\nu_{J_7} + C_8(j)\Delta\nu_{J_8} \\ & + C_9(j)\Delta\nu_{J_9} + C_{10}(j)\Delta\nu_{J_{10}} + C_{11}(j)\Delta\nu_{J_{11}} \end{aligned} \tag{13}$$

where j stands for the quantum number of spectrum lines to be predicted. There are 11 independent variables $(\Delta\nu_{J_1 \sim J_{11}})$ and $m > 11$ equations in Eq. (13). According to the principle of over determined linear equations, the error $\Delta v_{J_i} (i = 1\cdots11)$ can be estimated as $\Delta\nu_{J_i} = (C'C_i)^{-1} \times C'\sigma \ (i = 1\cdots11)$. Where $C_i (i = 1\cdots11)$ is the expansion coefficient, C' is the transposing of the C matrix and the σ is the difference between the experimental values and the theoretical calculation values. Once $\Delta v_{J_i} (i = 1\cdots11)$ are determined, one can use Eq. (12) estimate the error when predicting unknown experimental data by Eq. (11).

3. Application and Discussion

The improved analytical formula Eq. (7) is applied to predict the R-branch transition emission spectral lines of the (0–0) band of the $A_20^+ \rightarrow X_10^+$ and $A_20^+ \rightarrow X_21$ transition systems of BiLi molecule [21] in this study. Table 1 lists the corresponding rotational quantum numbers $(J_1 \cdots J_{11})$ of the 11 selected known experimental transition lines and shows the transition spectrum lines error $\Delta v_{J_i} (i = 1\cdots11)$ introduced by experiment and determined using Eqs. (12)–(13) for the (0–0) band of the $A_20^+ \rightarrow X_10^+$ and $A_20^+ \rightarrow X_21$ transition systems. It is worth mentioning that there are no any particular limitations about the rotational quantum numbers as long as the expansion coefficients $C_1 \sim C_{11} \neq 0$.

From Table 2, one can see that the rovibrational spectral lines calculated by Eq. (7) not only reproduce the given all m known experimental data, but also predict the data of new rovibrational spectral lines v_{Cal} up

Table 1
The rotational quantum numbers J_k and the error Δv_{J_k} values respectively corresponding to the 11 selected known experimental transition lines of (0–0) band of $A_20^+ \rightarrow X_10^+$ and $A_20^+ \rightarrow X_21$ transition systems of BiLi molecule.

$A_20^+ \rightarrow X_10^+$				$A_20^+ \rightarrow X_21$			
Band(0–0)							
J_1	2	Δv_{J_1}	0.3331	J_1	2	Δv_{J_1}	1.1442
J_2	6	Δv_{J_2}	−0.1556	J_2	6	Δv_{J_2}	0.1525
J_3	12	Δv_{J_3}	0.3641	J_3	7	Δv_{J_3}	1.1136
J_4	16	Δv_{J_4}	−0.1245	J_4	13	Δv_{J_4}	0.1219
J_5	17	Δv_{J_5}	0.3945	J_5	15	Δv_{J_5}	1.0831
J_6	24	Δv_{J_6}	−0.0940	J_6	20	Δv_{J_6}	0.0915
J_7	28	Δv_{J_7}	0.4256	J_7	30	Δv_{J_7}	1.0527
J_8	30	Δv_{J_8}	−0.0622	J_8	44	Δv_{J_8}	0.0610
J_9	34	Δv_{J_9}	0.4563	J_9	45	Δv_{J_9}	1.0222
J_{10}	50	$\Delta v_{J_{10}}$	−0.0324	J_{10}	46	$\Delta v_{J_{10}}$	0.0305
J_{11}	53	$\Delta v_{J_{11}}$	0.4872	J_{11}	59	$\Delta v_{J_{11}}$	0.9922

Table 2
Experimental and theoretical calculation transition lines of R-branch emission spectra of (0–0) band of the $A_20^+ \rightarrow X_10^+$ transition of BiLi (in cm^{-1}).

J	v_{Expt}	v_{Cal}	$v_{Expt} - v_{Cal}$	Δ_{Expt}	Δ_{Cal}	*Error%*	$\Delta\delta$
0	9184.5603	9184.5592	1.1154×10^{-3}			1.2144×10^{-5}	4.0069×10^{-4}
1	9185.3849	9185.3836	1.3354×10^{-3}			1.4538×10^{-5}	7.5657×10^{-4}
2	9186.2728	9186.2713	1.4809×10^{-3}	0.8879	0.8878	1.6120×10^{-5}	8.0969×10^{-4}
3	9187.224	9187.2224	1.6009×10^{-3}	0.9512	0.9511	1.7426×10^{-5}	9.7959×10^{-4}
4	9188.2384	9188.2368	1.6494×10^{-3}	1.0144	1.0144	1.7951×10^{-5}	1.1435×10^{-3}
5	9189.316	9189.3143	1.6844×10^{-3}	1.0776	1.0776	1.8330×10^{-5}	1.1272×10^{-3}
6	9190.4571	9190.4550	2.0685×10^{-3}	1.1411	1.1407	2.2507×10^{-5}	1.0478×10^{-3}
7	9191.6604	9191.6588	1.5687×10^{-3}	1.2033	1.2038	1.7066×10^{-5}	1.1019×10^{-3}
8	9192.9272	9192.9256	1.5565×10^{-3}	1.2668	1.2668	1.6932×10^{-5}	1.1614×10^{-3}
9	9194.2573	9194.2554	1.9082×10^{-3}	1.3301	1.3297	2.0754×10^{-5}	1.0659×10^{-3}
10	9195.6491	9195.6480	1.1052×10^{-3}	1.3918	1.3926	1.2019×10^{-5}	8.9821×10^{-4}
11	9197.1051	9197.1034	1.7349×10^{-3}	1.4560	1.4554	1.8863×10^{-5}	7.4752×10^{-4}
12	9198.6223	9198.6214	8.9157×10^{-4}	1.5172	1.5180	9.6924×10^{-6}	5.2104×10^{-4}
13	9200.2027	9200.2020	6.7826×10^{-4}	1.5804	1.5806	7.3722×10^{-6}	4.8588×10^{-4}
14	9201.8461	9201.8434	2.7381×10^{-3}	1.6434	1.6413	2.9756×10^{-5}	2.4374×10^{-3}
15	9203.551	9203.5518	-7.6836×10^{-4}	1.7049	1.7084	8.3485×10^{-6}	-1.0578×10^{-3}
16	9205.3191	9205.3176	1.4792×10^{-3}	1.7681	1.7659	1.6069×10^{-5}	1.0237×10^{-3}
17	9207.1488	9207.1485	3.0228×10^{-4}	1.8297	1.8309	3.2831×10^{-6}	-2.3827×10^{-4}
18	9209.0399	9209.0395	4.3422×10^{-4}	1.8911	1.8910	4.7152×10^{-6}	8.3664×10^{-4}
19	9210.994	9210.9950	-1.0312×10^{-3}	1.9541	1.9556	1.1195×10^{-5}	-1.3400×10^{-3}
20	9213.0102	9213.0102	1.9763×10^{-5}	2.0162	2.0151	2.1452×10^{-7}	-1.1578×10^{-3}
21	9215.0867	9215.0859	8.3931×10^{-4}	2.0765	2.0757	9.1080×10^{-6}	6.1588×10^{-4}
22	9217.2254	9217.2264	-1.0110×10^{-3}	2.1387	2.1406	1.0969×10^{-5}	-1.4223×10^{-3}
23	9219.4255	9219.4279	-2.3908×10^{-3}	2.2001	2.2015	2.5932×10^{-5}	-2.7342×10^{-3}
24	9221.6876	9221.6884	-8.3941×10^{-4}	2.2621	2.2605	9.1026×10^{-6}	-2.1142×10^{-3}
25	9224.0095	9224.0099	-4.1344×10^{-4}	2.3219	2.3215	4.4822×10^{-6}	-1.1261×10^{-3}
26	9226.3931	9226.3928	3.5211×10^{-4}	2.3836	2.3828	3.8163×10^{-6}	-2.5455×10^{-4}
27	9228.837	9228.8389	-1.9386×10^{-3}	2.4439	2.4462	2.1006×10^{-5}	-2.5459×10^{-3}
28	9231.3418	9231.3438	-2.0163×10^{-3}	2.5048	2.5049	2.1842×10^{-5}	-2.7536×10^{-3}
29	9233.9069	9233.9085	-1.5972×10^{-3}	2.5651	2.5647	1.7297×10^{-5}	-2.1169×10^{-3}
30	9236.5324	9236.5356	-3.1580×10^{-3}	2.6255	2.6271	3.4191×10^{-5}	-3.9218×10^{-3}
31	9239.2171	9239.2208	-3.6981×10^{-3}	2.6847	2.6852	4.0026×10^{-5}	-3.5653×10^{-3}
32	9241.9641	9241.9657	-1.5765×10^{-3}	2.7470	2.7449	1.7058×10^{-5}	-2.6287×10^{-3}
33	9244.7684	9244.7730	-4.5729×10^{-3}	2.8043	2.8073	4.9465×10^{-5}	-4.8322×10^{-3}
34	9247.6342	9247.6385	-4.3349×10^{-3}	2.8658	2.8656	4.6876×10^{-5}	-5.6644×10^{-3}
35	9250.5575	9250.5553	2.2387×10^{-3}	2.9233	2.9167	2.4201×10^{-5}	2.8948×10^{-3}
36	9253.5407	9253.5390	1.6656×10^{-3}	2.9832	2.9838	1.8000×10^{-5}	2.5392×10^{-3}
37	9256.5834	9256.5828	6.3835×10^{-4}	3.0427	3.0437	6.8962×10^{-6}	6.8139×10^{-4}
38	9259.6844	9259.6836	8.2688×10^{-4}	3.1010	3.1008	8.9299×10^{-6}	8.7791×10^{-4}
39	9262.8442	9262.8455	-1.2992×10^{-3}	3.1598	3.1619	1.4026×10^{-5}	-2.1033×10^{-3}
40	9266.0614	9266.0634	-2.0307×10^{-3}	3.2172	3.2179	2.1915×10^{-5}	-2.3091×10^{-3}
41	9269.3378	9269.3402	-2.4339×10^{-3}	3.2764	3.2768	2.6257×10^{-5}	-3.3437×10^{-3}
42	9272.6726	9272.6724	1.6771×10^{-4}	3.3348	3.3322	1.8086×10^{-6}	-1.7675×10^{-3}
43	9276.0629	9276.0606	2.2783×10^{-3}	3.3903	3.3882	2.4561×10^{-5}	1.9284×10^{-3}
44	9279.5123	9279.5103	2.0522×10^{-3}	3.4494	3.4496	2.2115×10^{-5}	9.6890×10^{-4}
45	9283.0163	9283.0206	-4.2950×10^{-3}	3.5040	3.5103	4.6268×10^{-5}	-4.2145×10^{-3}
46	9286.5796	9286.5804	-7.9004×10^{-4}	3.5633	3.5598	8.5073×10^{-6}	-1.0649×10^{-3}
47	9290.1995	9290.1991	4.4460×10^{-4}	3.6199	3.6187	4.7857×10^{-6}	-4.4752×10^{-5}
48	9293.8742	9293.8777	-3.5392×10^{-3}	3.6747	3.6787	3.8081×10^{-5}	-3.4579×10^{-3}
49	9297.6059	9297.6099	-3.9501×10^{-3}	3.7317	3.7321	4.2485×10^{-5}	-4.2319×10^{-3}
50	9301.3953	9301.3975	-2.2185×10^{-3}	3.7894	3.7877	2.3851×10^{-5}	-3.6943×10^{-3}
51	9305.2368	9305.2405	-3.6694×10^{-3}	3.8415	3.8430	3.9434×10^{-5}	-3.9331×10^{-3}
52	9309.1346	9309.1384	-3.8003×10^{-3}	3.8978	3.8979	4.0824×10^{-5}	-3.0618×10^{-3}
53	9313.0901	9313.0890	1.1417×10^{-3}	3.9555	3.9506	1.2259×10^{-5}	5.9399×10^{-4}
54		9317.0980			4.0091		-4.1694×10^{-4}
55		9321.1597			4.0616		9.7942×10^{-4}
56		9325.2811			4.1214		-4.1800×10^{-3}
57		9329.4530			4.1719		-5.9301×10^{-3}
58		9333.6772			4.2242		-5.7567×10^{-3}
59		9337.9572			4.2800		-8.6614×10^{-3}
60		9342.2840			4.3268		-4.3561×10^{-3}
61		9346.6655			4.3815		-2.2286×10^{-3}
62		9351.1031			4.4376		-5.1062×10^{-3}
63		9355.5903			4.4872		-5.4480×10^{-3}
64		9360.1318			4.5416		-8.5159×10^{-3}
65		9364.7232			4.5914		-9.4566×10^{-3}
66		9369.3647			4.6415		-9.7299×10^{-3}
67		9374.0561			4.6914		-9.7780×10^{-3}
68		9378.7990			4.7429		-1.0398×10^{-2}
69		9383.5893			4.7903		-8.7599×10^{-3}
70		9388.4335			4.8442		-1.1839×10^{-2}
71		9393.3245			4.8910		-1.2488×10^{-2}
72		9398.2639			4.9394		-1.2730×10^{-2}
73		9403.2550			4.9911		-1.6212×10^{-2}

(continued on next page)

Table 2 (*continued*)

J	ν_{Expt}	ν_{Cal}	$\nu_{Expt} - \nu_{Cal}$	Δ_{Expt}	Δ_{Cal}	*Error%*	$\Delta\delta$
74		9408.2918			5.0369		-1.7743×10^{-2}
75		9413.3773			5.0855		-1.9329×10^{-2}
76		9418.5104			5.1331		-2.2549×10^{-2}
77		9423.6899			5.1794		-2.4821×10^{-2}
78		9428.9128			5.2229		-1.9755×10^{-2}
79		9434.1908			5.2780		-3.3344×10^{-2}
80		9439.5081			5.3173		-3.4421×10^{-2}

to $J_{\max}^{Cal}$=80 for (0–0) band of the $A_20^+ \rightarrow X_10^+$system of BiLi. Separately, the maximum absolute spectral difference $|\nu_{Expt} - \nu_{Cal}|_{\max}^{J=19} = 2.7381 \times 10^{-3}\text{cm}^{-1}$ and the minimum absolute spectral difference $|\nu_{Expt} - \nu_{Cal}|_{\min}^{J=38} = -4.573 \times 10^{-3}\text{cm}^{-1}$ between the experimental and theoretical calculation data from Table 2 are illustrated in Fig. 1. And the maximum relative percent error $Error\%_{\max}^{J=19} = 2.7381 \times 10^{-3}$ the minimum relative percent error $Error\%_{\min}^{J=20} = 2.1452 \times 10^{-7}$. Comparatively, we found that the difference between the experimental differences and theoretical differences is in the range of −0.0063–0.0066 cm^{-1}. According to Eq. (12), the estimated transition spectrum lines error $\Delta\delta$between theoretical calculation values and real values are in Table 2, which tell us how accurate our prediction is and how many unknown lines we can predict reliably. The maximum absolute error is $\Delta\delta_{\max}^{J=80} = 3.442 \times 10^{-2}\text{cm}^{-1}$, the minimum absolute error is $\Delta\delta_{\min}^{J=47} = 4.475 \times 10^{-5}\text{cm}^{-1}$. The prediction error is controlled within the range of 10^{-2}cm^{-1}. Therefore, it shows that the predicted transition spectrum lines obtained by this method is very reliable.

Table 3 shows (0–0) transition of the $A_20^+ \rightarrow X_21$ system of BiLi. The maximum absolute spectral difference between experimental and theoretical data is $|\nu_{Expt} - \nu_{Cal}|_{\max}^{J=55} = 1.0543 \times 10^{-3}\text{cm}^{-1}$and the minimum absolute spectral difference is $|\nu_{Expt} - \nu_{Cal}|_{\min}^{J=16} = -1.0075 \times 10^{-3}\text{cm}^{-1}$, the maximum relative percent error is $Error\%_{\max}^{J=55} = 1.4032 \times 10^{-5}$ and the minimum relative percent error is $Error\%_{\min}^{J=7} = 6.0033 \times 10^{-7}$. The difference between the experimental and theoretical differences is in the range of −0.0012–0.0014 cm^{-1}. Form Table 3, the maximum absolute error $\Delta\delta$ between theoretical calculation values and real values is $\Delta\delta_{\max}^{J=79} = 6.113 \times 10^{-3}\text{cm}^{-1}$, the minimum absolute error is $\Delta\delta_{\min}^{J=37} = 1.531 \times 10^{-5}\text{cm}^{-1}$. Consequently, we have found that the calculating values not only reproduce the experimental values, but also calculate the low excited state transition line including ($J = 0$), which may not be available experimentally.

In order to intuitively understand the comparison, the experimental transition lines ("—") and the theoretical calculation transition lines ("——") are shown in Fig.2. The experimental difference ("o") and the theoretical differences ("+") for (0–0) transition band of the $A_20^+ \rightarrow X_10^+$ and $A_20^+ \rightarrow X_21$ systems of BiLi molecule are given in Figs. 3 and 4. The spectral difference between experimental transition lines and theoretical transition lines $\nu_{Expt} - \nu_{Cal}$ are shown in Fig. 1. The variations of the expansion coefficients C with the rotational quantum numbers J of the $A_20^+ \rightarrow X_10^+$ transition are shown in Fig. 5.

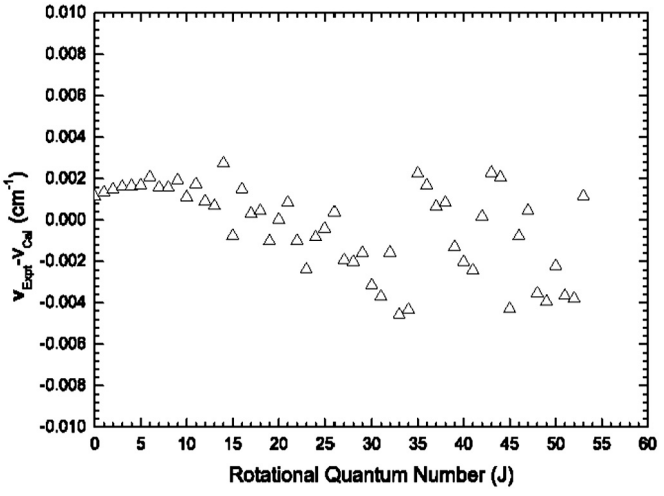

Fig. 1. The difference ($\nu_{Expt} - \nu_{Cal}$) between the experimental and theoretical calculation results of (0–0) band of the $A_20^+ \rightarrow X_10^+$ transition of BiLi.

It can be clearly seen from Figs. 1 and 2 that not only the ν_{Cal} and the ν_{Expt}agree well with each other, but also the predicted unknown high-lying rovibrational transition lines follow the physical trend of the band. The method used here can handle the doublet splitting spectral differences well.

From Eqs. (7) and (12) one can see that the error in calculating line $\nu_{J_{12}}$ is determined both by the uncertainty in experiment ($\nu_{J_{12}}$) and magnitude of C coefficients. They are linearly correlated. If C coefficients value is small the calculated error is small. The relation between the expansion coefficients and the rotational quantum numbers J are shown in Fig. 5. for the $A_20^+ \rightarrow X_10^+$ system. When the range of rotational quantum number $J < 58$, the expansion coefficients C_1~C_{11} are limited to −20–20. When nearby $J = 58$ they reach minimum. When $J > 58$ the absolute value of expansion coefficients are obviously enlarged with the increase of rotation quantum number. This is why high-lying rovibrational transition lines are difficult to predict from a mathematical point of view. We use Eq. (12) to handle the problem and the scope of the prediction can be extended to $J = 79$with an error less than $6.113 \times 10^{-3}\text{cm}^{-1}$. It is worth to note that $\{C_1, C_2, C_3, C_4, C_5, C_7\}$ variation tendency is significantly greater than other C values. Therefore, $\{C_1, C_2, C_3, C_4, C_5, C_7\}$ corresponding transition lines $\{\nu_1, \nu_2, \nu_3, \nu_4, \nu_5, \nu_7\}$ have a greater impact on the error of forecasting the high-lying vibrational states emission spectra. Fig. 6 shows very similar theoretical qualities and behavior as those in Fig. 5 for the $A_20^+ \rightarrow X_21$ system. Any improvements in experimental accuracy are obviously also helpful to increasing the accuracy of the calculated lines.

4. Summary

In order to predict unknown rotational lines of diatomic molecule more conveniently and accurately, a new analytical formula without any spectral constants is derived from the conventional expression of R-branch transitional energies with higher terms including rovibrational constants L_v. Using the formula, based on the difference converging method (DCM), only a set of 11 known R-branch experimental transition spectral lines are needed to predict reliable high-lying transitional spectra that may not be available experimentally. More importantly, we find the reason why the high quantum number spectrum is difficult to predict from another mathematical point view, and construct a method of estimating prediction uncertainty by further analysis. The method is applied to calculate high-lying rovibrational spectral lines of the R-branch emission spectral lines of the (0–0) band of the $A_20^+ \rightarrow X_10^+$ and $A_20^+ \rightarrow X_21$ systems of BiLi molecule. The results not only verify the effectiveness of our method, but also provide a data reference for future study the physical and chemical properties of BiLi.

Table 3
Experimental and theoretical calculation transition lines of R-branch emission spectra of (0–0) band of the $A_20^+ \rightarrow X_21$ transition of BiLi (in cm^{-1}).

J	v_{Expt}	v_{Cal}	$v_{Expt} - v_{Cal}$	Δ_{Expt}	Δ_{Cal}	$Error\%$	$\Delta\delta$
0		7412.6718					7.5020×10^{-4}
1	7413.4724	7413.4725	-8.5190×10^{-5}			1.1491×10^{-6}	7.4005×10^{-4}
2	7414.3126	7414.3127	-8.2995×10^{-5}	0.8402	0.8402	1.1194×10^{-6}	7.4708×10^{-4}
3	7415.1922	7415.1923	-1.2020×10^{-4}	0.8796	0.8796	1.6210×10^{-6}	6.4259×10^{-4}
4	7416.1113	7416.1114	-5.5153×10^{-5}	0.9191	0.9190	7.4369×10^{-7}	4.9015×10^{-4}
5	7417.0697	7417.0697	-4.3897×10^{-5}	0.9584	0.9584	5.9184×10^{-7}	3.9902×10^{-4}
6	7418.0674	7418.0674	-4.0205×10^{-5}	0.9977	0.9977	5.4198×10^{-7}	5.2118×10^{-4}
7	7419.1044	7419.1044	4.4539×10^{-6}	1.0370	1.0370	6.0033×10^{-8}	3.2357×10^{-4}
8	7420.1806	7420.1806	4.0924×10^{-5}	1.0762	1.0762	5.5153×10^{-7}	3.2408×10^{-4}
9	7421.2959	7421.2959	2.2398×10^{-5}	1.1153	1.1153	3.0181×10^{-7}	2.9730×10^{-4}
10	7422.4503	7422.4503	4.4560×10^{-6}	1.1544	1.1544	6.0034×10^{-8}	2.8208×10^{-4}
11	7423.6438	7423.6438	4.5130×10^{-5}	1.1935	1.1935	6.0792×10^{-7}	3.7296×10^{-4}
12	7424.8762	7424.8762	7.9287×10^{-6}	1.2324	1.2324	1.0679×10^{-7}	1.3098×10^{-4}
13	7426.1476	7426.1476	5.0185×10^{-5}	1.2714	1.2714	6.7579×10^{-7}	2.8848×10^{-4}
14	7427.4578	7427.4578	4.0851×10^{-5}	1.3102	1.3102	5.5001×10^{-7}	1.3951×10^{-4}
15	7428.8069	7428.8068	9.4844×10^{-5}	1.3491	1.3490	1.2767×10^{-6}	3.6477×10^{-4}
16	7430.1935	7430.1945	-1.0075×10^{-3}	1.3866	1.3877	1.3559×10^{-5}	1.4770×10^{-4}
17	7431.6206	7431.6209	-2.9861×10^{-4}	1.4271	1.4264	4.0180×10^{-6}	2.6418×10^{-4}
18	7433.0866	7433.0858	7.5805×10^{-4}	1.4660	1.4649	1.0198×10^{-5}	1.8177×10^{-4}
19	7434.5887	7434.5893	-6.1074×10^{-4}	1.5021	1.5035	8.2148×10^{-6}	2.0791×10^{-4}
20	7436.1313	7436.1312	1.3763×10^{-4}	1.5426	1.5419	1.8509×10^{-6}	1.1639×10^{-4}
21	7437.7114	7437.7114	4.5897×10^{-5}	1.5801	1.5802	6.1708×10^{-7}	1.6736×10^{-4}
22	7439.3299	7439.3299	5.3956×10^{-5}	1.6185	1.6185	7.2528×10^{-7}	2.8183×10^{-4}
23	7440.9867	7440.9865	1.7139×10^{-4}	1.6568	1.6567	2.3034×10^{-6}	1.0349×10^{-4}
24	7442.6817	7442.6812	4.7542×10^{-4}	1.6950	1.6947	6.3877×10^{-6}	2.1175×10^{-4}
25	7444.4142	7444.4139	2.7208×10^{-4}	1.7325	1.7327	3.6548×10^{-6}	8.2478×10^{-5}
26	7446.1846	7446.1846	4.0192×10^{-5}	1.7704	1.7706	5.3977×10^{-7}	1.5340×10^{-4}
27	7447.9933	7447.9930	2.7563×10^{-4}	1.8087	1.8085	3.7007×10^{-6}	1.9418×10^{-4}
28	7449.8392	7449.8393	-7.7546×10^{-5}	1.8459	1.8463	1.0409×10^{-6}	-1.1942×10^{-4}
29	7451.7231	7451.7230	6.3021×10^{-5}	1.8839	1.8838	8.4573×10^{-7}	-3.1967×10^{-4}
30	7453.6444	7453.6443	7.2575×10^{-5}	1.9213	1.9213	9.7369×10^{-7}	-2.0218×10^{-4}
31	7455.6032	7455.6032	-2.8254×10^{-5}	1.9588	1.9589	3.7896×10^{-7}	-2.3175×10^{-4}
32	7457.5991	7457.5992	-1.2010×10^{-4}	1.9959	1.9960	1.6104×10^{-6}	-1.3363×10^{-4}
33	7459.6321	7459.6324	-3.4106×10^{-4}	2.0330	2.0332	4.5721×10^{-6}	-9.8780×10^{-5}
34	7461.7027	7461.7027	-2.1588×10^{-5}	2.0706	2.0703	2.8932×10^{-7}	-1.3944×10^{-4}
35	7463.8102	7463.8100	2.2560×10^{-4}	2.1075	2.1073	3.0225×10^{-6}	-1.1647×10^{-4}
36	7465.9538	7465.9541	-2.7716×10^{-4}	2.1436	2.1441	3.7123×10^{-6}	-2.7258×10^{-5}
37	7468.1345	7468.1349	-4.2879×10^{-4}	2.1807	2.1809	5.7416×10^{-6}	-1.5315×10^{-5}
38	7470.3522	7470.3524	-1.8267×10^{-4}	2.2177	2.2175	2.4452×10^{-6}	-4.3953×10^{-5}
39	7472.6064	7472.6064	3.7754×10^{-5}	2.2542	2.2540	5.0524×10^{-7}	1.2446×10^{-4}
40	7474.8967	7474.8967	1.4602×10^{-5}	2.2903	2.2903	1.9535×10^{-7}	1.9846×10^{-4}
41	7477.2231	7477.2236	-5.1911×10^{-4}	2.3264	2.3269	6.9425×10^{-6}	-2.4034×10^{-4}
42	7479.5864	7479.5864	5.0036×10^{-5}	2.3633	2.3627	6.6896×10^{-7}	2.9935×10^{-5}
43	7481.9853	7481.9850	2.8175×10^{-4}	2.3989	2.3987	3.7657×10^{-6}	-3.2526×10^{-5}
44	7484.4198	7484.4196	2.2508×10^{-4}	2.4345	2.4346	3.0073×10^{-6}	-1.3038×10^{-4}
45	7486.8901	7486.8901	-1.5085×10^{-5}	2.4703	2.4705	2.0149×10^{-7}	4.1680×10^{-5}
46	7489.3961	7489.3961	2.7705×10^{-5}	2.5060	2.5060	3.6992×10^{-7}	-1.5432×10^{-4}
47	7491.9383	7491.9374	9.3608×10^{-4}	2.5422	2.5413	1.2494×10^{-5}	1.1340×10^{-4}
48	7494.5137	7494.5142	-4.8680×10^{-4}	2.5754	2.5768	6.4955×10^{-6}	-2.4986×10^{-5}
49	7497.1259	7497.1261	-1.5288×10^{-4}	2.6122	2.6119	2.0392×10^{-6}	2.7660×10^{-5}
50	7499.7730	7499.7731	-4.5428×10^{-5}	2.6471	2.6470	6.0573×10^{-7}	5.4513×10^{-5}
51	7502.4551	7502.4548	3.5126×10^{-4}	2.6821	2.6817	4.6819×10^{-6}	1.4945×10^{-4}
52	7505.1713	7505.1713	5.1784×10^{-5}	2.7162	2.7165	6.8997×10^{-7}	1.1118×10^{-4}
53	7507.9214	7507.9222	-8.2549×10^{-4}	2.7501	2.7510	1.0995×10^{-5}	-2.7574×10^{-5}
54	7510.7076	7510.7077	-1.1151×10^{-4}	2.7862	2.7855	1.4847×10^{-6}	2.3013×10^{-4}
55	7513.5286	7513.5276	1.0543×10^{-3}	2.8210	2.8198	1.4032×10^{-5}	3.3834×10^{-4}
56	7516.3816	7516.3814	1.6888×10^{-4}	2.8530	2.8539	2.2468×10^{-6}	2.6446×10^{-4}
57	7519.2695	7519.2692	2.9651×10^{-4}	2.8879	2.8878	3.9433×10^{-6}	1.2044×10^{-4}
58	7522.1913	7522.1907	5.6016×10^{-4}	2.9218	2.9215	7.4468×10^{-6}	2.4933×10^{-4}
59	7525.1457	7525.1459	-1.5251×10^{-4}	2.9544	2.9551	2.0266×10^{-6}	3.7963×10^{-4}
60		7528.1344			2.9885		5.2420×10^{-4}
61		7531.1561			3.0217		7.5315×10^{-4}
62		7534.2111			3.0550		7.1226×10^{-4}
63		7537.2989			3.0878		7.7150×10^{-4}
64		7540.4194			3.1206		1.0937×10^{-3}
65		7543.5724			3.1529		1.0882×10^{-3}
66		7546.7579			3.1855		1.1349×10^{-3}
67		7549.9754			3.2175		1.7609×10^{-3}
68		7553.2250			3.2496		1.7377×10^{-3}
69		7556.5067			3.2817		1.2046×10^{-3}
70		7559.8196			3.3129		1.6703×10^{-3}
71		7563.1640			3.3445		2.3289×10^{-3}
72		7566.5398			3.3757		2.4314×10^{-3}
73		7569.9465			3.4067		2.5627×10^{-3}
74		7573.3839			3.4374		2.8503×10^{-3}

(continued on next page)

Table 3 (*continued*)

J	ν_{Expt}	ν_{Cal}	$\nu_{Expt} - \nu_{Cal}$	Δ_{Expt}	Δ_{Cal}	Error%	$\Delta\delta$
75		7576.8523			3.4684		3.8529×10^{-3}
76		7580.3508			3.4985		3.4169×10^{-3}
77		7583.8796			3.5288		4.2065×10^{-3}
78		7587.4383			3.5587		4.5194×10^{-3}
79		7591.0270			3.5886		6.1130×10^{-3}
80		7594.6449			3.6179		4.3774×10^{-3}

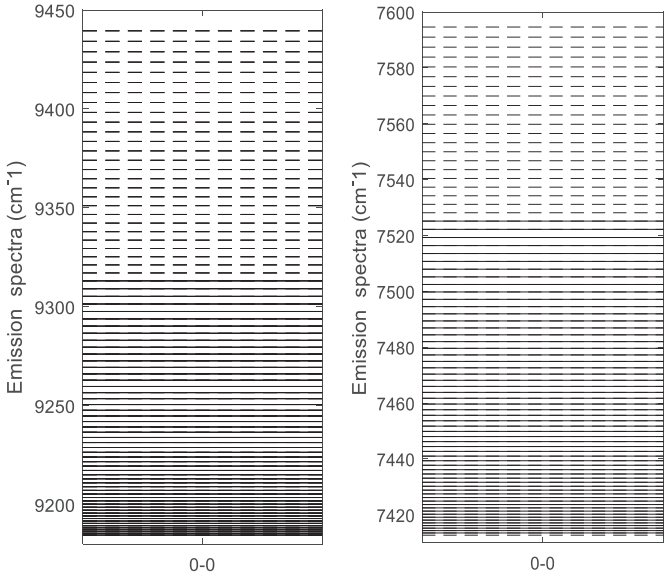

Fig. 2. Experimental ("—") and theoretical calculation ("—") transition lines of R-branch emission spectra of (0–0) band of the $A_20^+ \rightarrow X_10^+$ and $A_20^+ \rightarrow X_21$ transitions of BiLi.

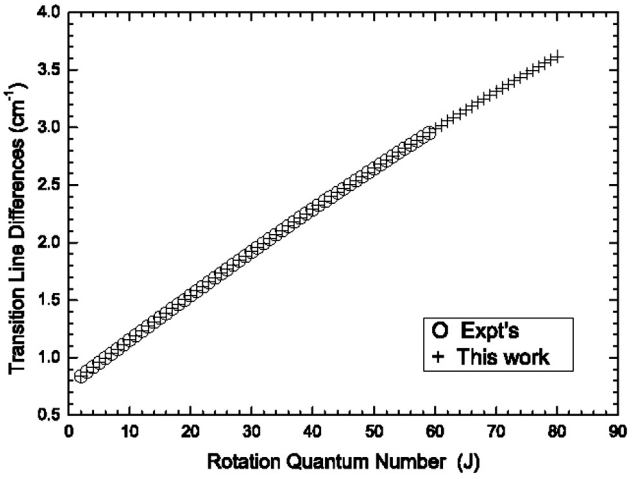

Fig. 4. Experimental ("o") and theoretical calculation("+") transition lines differences ($\Delta_J = \nu_{J-1} - \nu_J$) of R-branch transitional emission spectral lines of (0–0) band of the $A_20^+ \rightarrow X_21$ transition of BiLi.

Acknowledgements

The work was supported by the Chunhui Plan of the Chinese Educational Ministry under Grant No. Z2016160, the National Natural Science Foundation of China (Nos. 11647058, 11605143, 91436108 and 61378014)

Appendix A. Supplementary data

Supplementary data to this article can be found online at https://doi.org/10.1016/j.saa.2018.03.082.

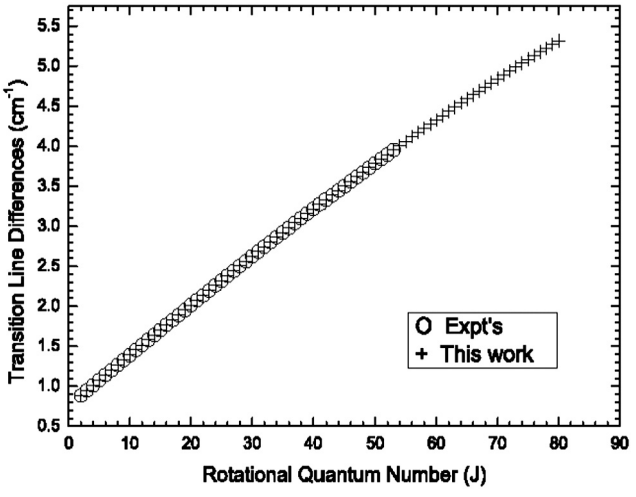

Fig. 3. Experimental ("o") and theoretical calculation ("+") transition lines differences ($\Delta_J = \nu_{J-1} - \nu_J$) of R-branch transitional emission spectral lines of (0–0) band of the $A_20^+ \rightarrow X_10^+$ transition of BiLi.

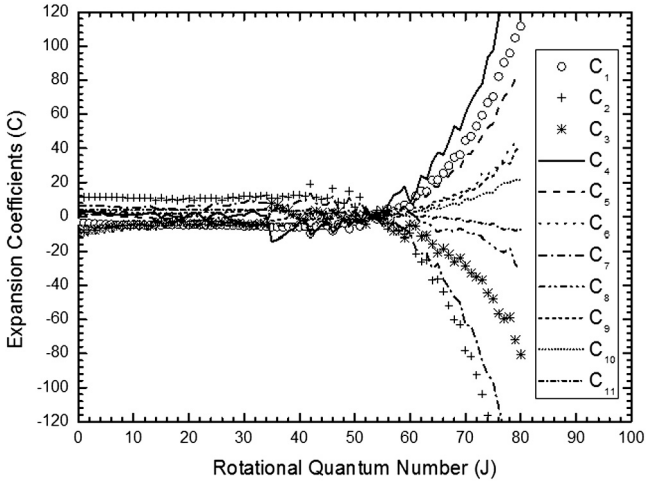

Fig. 5. The variations of the expansion coefficients C with the rotational quantum numbers J of (0–0) band of the $A_20^+ \rightarrow X_10^+$ transition of BiLi.

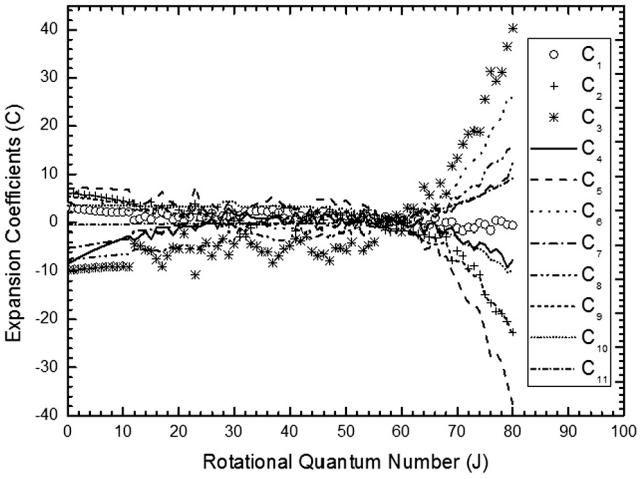

Fig. 6. The variations of the expansion coefficients *C* with the rotational quantum numbers *J* of (0–0) band of the $A_20^+ \rightarrow X_21$ transition of BiLi.

References

[1] R. Wynar, R.S. Freeland, D.J. Han, C. Ryu, D.J. Heinzen, Molecules in a Bose-Einstein condensate, Science 287 (2000) 1016–1019.

[2] C. Puzzarini, M.P. de Lara-Castells, R. Tarroni, P. Palmieri, J. Domaison, Accurate abinitio rediction of the rovibrational energy levels and equilibrium geometry of carbonyl selenide (OCSe), Phys. Chem. Chem. Phys. 1 (1999) 3955–3960.

[3] H.Z. Li, C. Focsa, B. Pinchemel, R.J. Le, P.F. Bernath Roy, Fourier transform spectroscopy of BaO: new ground-state constants from the A1Σ+–X1Σ+ chemiluminescence, J. Chem. Phys. 113 (2000) 3026–3033.

[4] Y. Huang, J. Qi, H.K. Pechkis, D. Wang, E.E. Eyler, P.L. Gould, W.C. Stwalley, Formation, detection and spectroscopy of ultracold Rb2 in the ground X1Σg+ state, J. Phys. B. 39 (2006) S857–S869.

[5] R.M. Herman, J.F. Ogilvie, An Effective Hamiltonian to Treat Adiabatic and Nonadiabatic Effects in the Rotational and Vibrational Spectra of Diatomic Molecules, John Wiley and Sons, Inc, 2007.

[6] R.C. Ekey Jr., A. Marks, E.F. McCormack, Double resonance spectroscopy of the B″B¯ 1Σ u+ state of H2, Phys. Rev. A 73 (2006) 023412.1–023412.5.

[7] F. Lang, K. Winkler, C. Strauss, R. Grimm, J.H. Denschlag, Ultracold triplet molecules in the rovibrational ground state, Phys. Rev. Lett. 101 (2008) 133005.1–133005.4.

[8] L.J. Zheng, X.H. Yang, L. Wu, K. Kaniki, Y.C. Guo, Y.Y. Liu, Y.Q. Chen, Rotational analysis of (6, 20), (4, 20), and (2, 18) bands in the second negative (A2Πu–X2Πg) system of 16O2+ cation, J. Mol. Spectrosc. 229 (2005) 131–136.

[9] J.J. Lutz, J.M. Hutson, Deviations from Born-Oppenheimer mass scaling in spectroscopy and ultracold molecular physics, J. Mol. Spectrosc. 330 (2016) 43–56.

[10] D. Borsalino, B. Londoño-Florèz, R. Vexiau, O. Dulieu, N. Bouloufa-Maafa, E. Luc-Koenig, Efficient optical schemes to create ultracold KRb molecules in their rovibronic ground state, Phys. Rew. A. 90 (2014) 033413.1–033413.14.

[11] M. Deiß, B. Drews, J.H. Denschlag, N. Bouloufa-Maafa, R. Vexiau, O. Dulieu, Polarizability of ultracold Rb2 molecules in the rovibrational ground state of a3Σ̃u+, New J. Phys. 17 (2015) 065019.1–065019.14.

[12] D. Ityaksov, S. Stolte, H. Linnartz, W. Ubachs, Rotational analysis of the A2Σ+(v = 1,2)-X2Π(v = 0) electronic bands of 15N18O, J. Mol. Spectrosc. 255 (2009) 139–143.

[13] L.N. Zack, R.L. Pulliam, L.M. Ziurys, The pure rotational spectrum of ZnO in the X1Σ̃+ and a3Πi states, J. Mol. Spectrosc. 256 (2009) 186–191.

[14] L.C. O'Brien, B.A. Borchert, A. Farquhar, S. Shaji, J.J. O'Brien, R.W. Field, Intracavity laser absorption spectroscopy of AuO: identification of the B2Σ-–X2Π3/2 transition, J. Mol. Spectrosc. 252 (2008) 136–142.

[15] K.O. Douglass, J.C. Keske, F.S. Rees, K. Welch, H.S. Yoo, B.H. Pate, I. Leonov, R.D. Suenram, Rotational spectroscopy of vibrationally excited states by infrared-Fourier transform microwave–microwave triple-resonance spectroscopy, Chem. Phys. Lett. 376 (2003) 548–556.

[16] J.A. Pople, P.M.W. Gill, B.G. Johnson, Kohn-Sham density-functional theory within a finite basis set, Chem. Phys. Lett. 199 (1992) 557–560.

[17] P.J. Knowles, H.J. Werner, An efficient second-order MC SCF method for long configuration expansions, Chem. Phys. Lett. 115 (1985) 259–267.

[18] W.G. Sun, Q.C. Fan, H.D. Li, H. Feng, Studies on the P-branch spectral lines of rovibrational transitions of diatomic system, Spectrochim. Acta A 79 (2011) 35–38.

[19] Y.H. Jiang, W.G. Sun, Y. Zhang, J. Fu, Q.C. Fan, H.D. Li, H. Feng, Prediction of P-branch emission spectral lines of NaF and 63Cu35Cl molecules, Spectrochim. Acta A 153 (2016) 87–93.

[20] A. Neubert, H.R. Ihle, K.A. Gingerich, Thermodynamic study of the molecules BiLi and PbLi by Knudsen effusion mass spectrometry, J. Chem. Phys. 73 (1980) 1406–1409.

[21] K.D. Setzer, E.H. Fink, H.-P. Liebermann, R.J. Buenker, A.B. Alekseyev, Experimental and theoretical study of the electronic states and spectra of BiLi, J. Mol. Spectrosc. 312 (2015) 38–45.

[22] A. Neubert, H.R. Ihle, K.A. Gingerich, Atomization energies of gaseous molecules of Li with Bi and Pb, J. Chem. Phys. 76 (1982) 2687–2692.

[23] J. Sangster, A.D. Pelton, The Bi-Li (Bismuth-Lithium) system, J. Phase. Equilibria. 12 (1991) 447–450.

[24] V. Pavlyuk, M. Sozanskyi, G. Dmytriv, S. Indris, H. Ehrenberg, Amendment of the Li-Bi phase diagram crystal and electronic structure of Li2Bi, J. Phase Equilib. Diffus. 36 (2015) 544–553.

[25] G. Herzeberg, Molecular Spectra and Molecular Structure (I): Spectra of Diatomic Molecules, Nostrand D Van Printing, New York, 1953.